

Reliable in vivo shimming for solving shim degeneracy and incorporating system constraints at high B₀ fields

Iulius Dragonu¹, Nicoleta Baxan^{1,2}, Markus Wick², Jeff Snyder³, Franek Hennel², Juergen Hennig¹, Dominik von Elverfeldt¹, and Maxim Zaitsev¹

¹Dept. Radiology - Medical Physics, University Medical Center Freiburg, Freiburg, Germany, ²Bruker BioSpin MRI GmbH, Ettlingen, Germany, ³Dept. of Neurology, University Medical Center Freiburg, Freiburg, Germany

Purpose: Discontinuities in the magnetic susceptibility generate induction fields which perturb the static B₀ field. At high B₀ fields the susceptibility difference effects are enhanced leading to potential shimming problems. Previously, several different approaches for in vivo shimming have been proposed [1, 2]. The corrective currents for the spherical harmonic shim coils can be calculated after acquisition of B₀ field maps. The problem of finding the correct shim values can become ill-conditioned for very thin or off-centred volumes. In such cases, the required linear independence of shim functions is not maintained leading to shim degeneracy [3]. Kim *et al.* introduced a regularized method for inversion of the shim matrix to address the numerical instability of an ill-conditioned inversion problem [4]. In this work, we propose a new method for solving the shim degeneracy problem in order to calculate the correct shim values. In addition, this technique will optimize the shim currents taking into account the limitations of the maximum current available for each shim channel.

Methods: All animal experiments were performed on a 9.4 T Bruker BioSpin scanner. Field maps spanning the entire rat brain were acquired with a dual-echo, 3D GRE sequence TE₁ = 2.5 ms, TE₂ = 3.9 ms with an acquisition time of 3 min 25 sec. The shim currents can be computed to minimize the mean squared residual ΔB₀ inhomogeneity inside a desired volume using the following relationships: $S \cdot I = \Delta B_0$ (1); $I = (S^T \cdot S)^{-1} \cdot S^T \cdot \Delta B_0$ (2), where S represents the shim matrix containing the shim coil values for an unitary current inside the volume chosen by the user. One possibility for detecting the shim degeneracy is the singular value decomposition of the shim matrix (Fig. 1). A poor condition number of this matrix indicates one or several interactions between different shims, and consequently, we propose to modify the initial cuboidal volume chosen by the user in the direction of the smallest dimension. However, in order to perform an improved optimization inside the initial user-defined volume, Eq. 2 is replaced with a weighted mean squared minimization: $I = (S^T \cdot W \cdot S)^{-1} \cdot S^T \cdot W \cdot \Delta B_0$ (3) with W being a diagonal weighting matrix with ones corresponding to the voxels inside the initial volume and 0.05 corresponding to the neighbouring voxels added automatically by the algorithm. Nevertheless, in regions with very high B₀ inhomogeneities the maximum current can be exceeded. In this case, the non-constrained minimizations from (2) and (3) have to be replaced with a constrained least square minimization. Two limitations are encountered on our system: 1) the maximum available current for each shim channel ($I_n \leq I_{nMAX}$) and 2) as the higher-order shims are driven by the same power supply, the sum of the absolute values of higher-order shims is constrained by the maximum available current of the power supply: $|I_k| + |I_{k+1}| + \dots + |I_{Nshims}| \leq I_{MAX}$ (4). All five second-order shims are driven by a single power supply with a maximum current of 20 A. The maximum available current for each shim channel is displayed in Table 1 second row.

For the constrained least square minimization, the active set algorithm was implemented on our system in the field map based shimming method. One constraint is considered active when equality occurs. For this algorithm the different constraints presented earlier have to be represented in a matrix form leading to a constraint matrix. The constraint matrix has a number of columns equal to the number of available shim channels. It contains in columns corresponding to the second order shims all possible combinations (32 possibilities for five shims) of -1 and 1. The constraint matrix is concatenated with ± the identity matrix in order to take into account the maximum available current for each shim channel. The active set algorithm is represented in Fig. 2.

Results/Discussion: In order to test the method in the most severe cases, we used initial volumes of (1.875×1.875×0.625 mm³) corresponding to a volume of 3×3×1 voxels with transverse orientation. Since shim degeneracy was observed in each case, this volume was increased to 3×3×3 voxels. The centre of each volume was chosen to ensure at least one of the voxels inside coincided with the border of the segmentation mask. 1408 different volumes were obtained on the border of the segmentation mask. The shim current values were first calculated using an unconstrained weighted least squares minimization (Eq.3). In 33.81% of the cases one of the constraints was not respected. For this particular setup, the maximum current for the Z2 shim was the constraint that was most often violated by the unconstrained minimization. Table 1 displays two representative results for the shim currents expressed in percentage of maximum available current for each channel indicated in the second row. The first example (Row 3 – unconstrained and Row 4 - constrained) shows an example of the violated constraint of the Z2-shim current. The constrained minimization shows that the limitation of the Z2 current is mainly compensated by significant modifications of Y-, Z- and YZ-shims. For the last example in Row 5 and 6, three maximum current constraints were violated as well as the sum of the currents (20 A). The constrained optimization (Row 6) achieves a solution where four constraints were reached (Z2 XZ 2XY as well as the sum of the currents). The proposed method

X	Y	Z	Z2	X2-Y2	XZ	YZ	2XY
15 A	15 A	15 A	5 A	5 A	5 A	5 A	5 A
11.9864	-9.1645	-20.4788	215.5664	-2.7417	36.7539	2.4142	2.2098
9.7170	-3.7330	-9.9566	100.0000	-4.4017	37.3417	14.0891	2.1705
-42.4058	7.0333	-7.1546	254.1612	40.3181	-123.7674	-28.3474	216.0656
-19.0391	8.3970	0.5008	100.0000	43.5821	-100.0000	-56.4179	100.0000

Table 1: Representative shim currents at the air/tissue interface for a 1.875×1.875×0.625 mm³ volume with and without constraints.

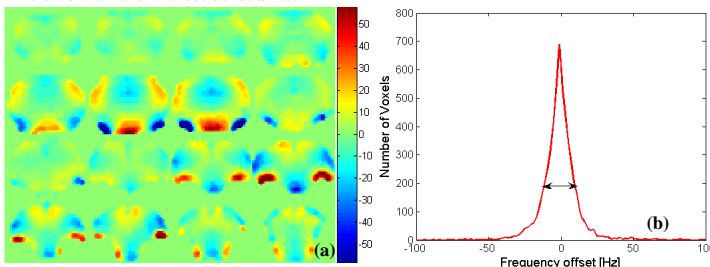


Figure 3: (a) Residual B₀ inhomogeneity for 16 representative slices; (b) Frequency offset histogram with 80% width of the distribution labelled.

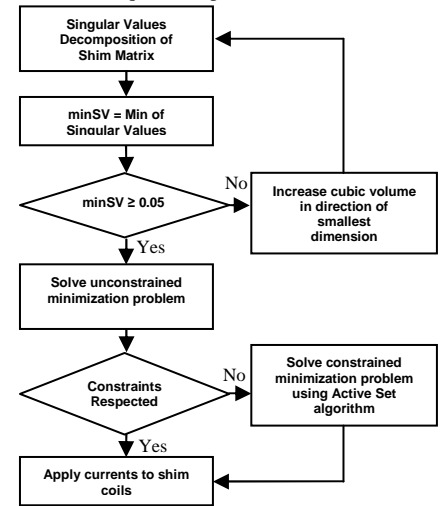


Figure 1: Schematic diagram of the proposed constrained shimming method.

```

while
I(k), λ ← quadratic problem (S, ΔB0, ...
ConstraintMatrix(Active Set),
ConstrainedValues(ActiveSet))
D(k) = I(k) - I(k-1)
If D(k) == 0
  if all λ are positive
    break
  else // (one λ is negative)
    remove constraint corresponding to min(λ)
else // (Dk ≠ 0)
  if I(k) found using the quadratic problem
    respects all constraints
    move to I(k)
  else
    I(k) = I(k-1) + α · D(k)
    0 < α < 1 determined by the most
    blocking constraint
  
```

Figure 2: Active set algorithm.

was also used to calculate the shim currents for each slice of the volume. Shim degeneracy in a single slice was solved by incorporating information from the two neighbouring slices only using the weighted mean (Eq. 3). In this particular experiment, only the Z2-shim was violated in the frontal brain for the first slice which was successfully solved by the constrained optimization. Figure 3a displays the residual inhomogeneity for 16 representative slices through the rat brain. The frequency offset histogram collected from the entire brain (manual segmentation) is represented in Fig. 3b.

Conclusion: The method presented here allows calculating reliable shim values for very small volumes; it solves the ill-conditioned shimming problem in cases of shim degeneracy and determines the optimal shim values taking into account the shim system limitations. Furthermore the method presented here was reliable and completely automated.

References: [1] Gruetter R, MRM 1993; 29:804-811. [2] Shen J *et al.*, MRM 1997; 38:834-839. [3] Koch KM *et al.*, JMR 2006; 180:286-296. [4] Kim D-H *et al.*, MRM 2002; 48:715-722. **Acknowledgements:** This work is a part of the INUMAC project supported by the German Federal Ministry of Education and Research, grant #01EQ0605.